

Behavior of atomic radicals and their effects on organic low dielectric constant film etching in high density N_2/H_2 and N_2/NH_3 plasmas

Hisao Nagai

Department of Quantum Engineering, Nagoya University, Furo-cho, Chikusa-ku, Nagoya 464-8603, Japan

Seigou Takashima

Nippon Laser & Electronics LAB, 20-9, Sanbonmatsu-cho, Atsuta-ku, Nagoya 456-0032, Japan

Mineo Hiramatsu

Department of Electrical and Electronic Engineering, Meijo University 1-501 Shiogamaguchi, Tempaku-ku, Nagoya 468-8502, Japan

Masaru Hori^{a)} and Toshio Goto

Department of Quantum Engineering, Nagoya University, Furo-cho, Chikusa-ku, Nagoya 464-8603, Japan

(Received 27 August 2001; accepted for publication 15 November 2001)

An organic film, FLARETM, is one of the most prospective candidates for interlayer insulating films with low dielectric constants (low k). This organic low k film was etched in inductively coupled high-density plasmas employing N_2/H_2 and N_2/NH_3 gases. By changing the mixing ratio of these gases, the anisotropic etching profile was obtained. The etching plasmas were evaluated by quadruple mass spectroscopy and the vacuum ultraviolet absorption spectroscopy employing microplasma as a light source. N and H radical densities were estimated on the order of 10^{11} – 10^{12} cm^{-3} and 10^{12} – 10^{13} cm^{-3} , respectively. The behavior of etch rate corresponded well to that of H radical density. H radicals were found to be important species for organic low k film etching, while N radicals could not etch without ion bombardments. On the other hand, N radicals were found to be effective for the formation of protection layer on the sidewall against the etching by the H radicals. The ratio of H and N radical densities would be important for the etching of organic low k film employing N–H plasmas. © 2002 American Institute of Physics.

[DOI: 10.1063/1.1435825]

I. INTRODUCTION

As the critical dimension of integrated circuits is scaled down, the linewidth and space between metal interconnections becomes smaller. A larger portion of the total circuit transmission time (i.e., RC delay) is expected due to the increase of the parasitic resistance (R) and capacitance (C) of interconnections. Therefore, this large portion becomes a bottleneck for improving the chip performance such as speed and power consumption. To address this issue, the combination of copper wiring of relatively low resistivity and interlayer films with lower dielectric constants (low k) has been proposed. Many researchers have investigated various kinds of organic,^{1–4} inorganic,⁵ and hybrid materials⁶ as an alternative to conventional interlayer dielectric films of SiO_2 ($k=4.0$). An organic low k film, FLARETM (Honeywell), has low dielectric constant ($k=2.85$), good thermal stability (450 °C) and good adhesion, and is considered to be one of the most prospective candidates for interlayer films with lower dielectric constant used in ultralarge scale integrated (ULSI) devices in the next generation. The etching process for the organic low k films should be performed without employing perfluorocarbon gases such as C_4F_8 of high global warming potential values. So far, it has been reported that N_2/H_2 and NH_3 plasmas are used for etching organic low k

films without degrading the film quality and the etched profile.^{3,4} In order to achieve the highly precise etching for the ULSI devices in the next generation, the etching mechanism of the organic low k films should be clarified. However, behaviors of H and N atoms have not been clarified enough. Recently, our group developed a measurement system of the H^7 and N^8 atom densities using vacuum ultraviolet absorption spectroscopy (VUVAS) with microdischarge hollow-cathode lamp (MHCL).

In this study, organic low k films were etched in inductively coupled high-density plasmas (ICP) employing N_2/H_2 and N_2/NH_3 gases. Moreover, the VUVAS technique was applied to measure the absolute densities of H and N atoms during etching of organic low k films. The correlation between the behaviors of H and N atom densities in high-density plasmas and the etching characteristics of organic low k film was investigated. On the basis of these results, the mechanism of anisotropic etching of organic low k films was discussed.

II. EXPERIMENT

Figure 1 shows a schematic diagram of ICP reactor equipped with the VUVAS system employing MHCL. The ICP chamber was 40 cm in diameter and 30 cm in height. A one-turn coil antenna with a diameter of 30 cm was set on a quartz window at the top of the chamber. Plasma power operating at 13.56 MHz was applied to a coil antenna and plasma was created in the chamber. The substrate as an etch-

^{a)}Electronic mail: hori@nuee.nagoya-u.ac.jp

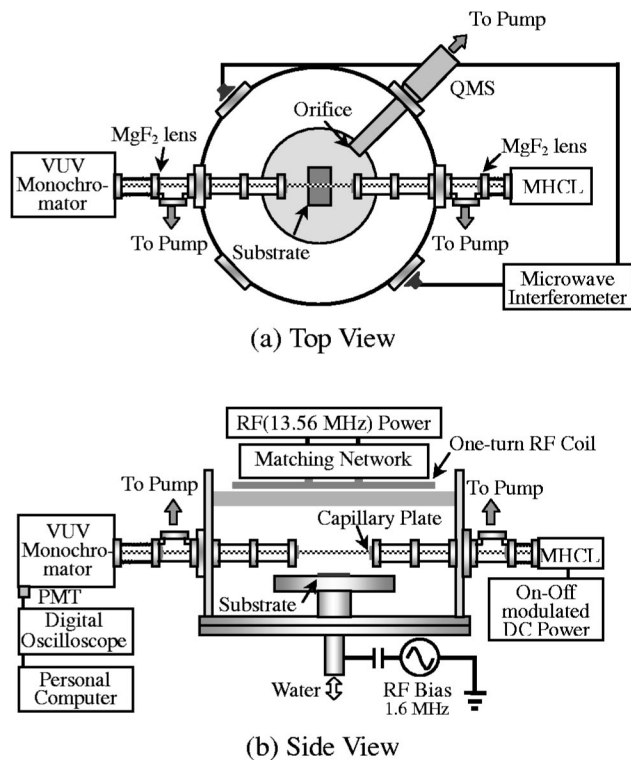


FIG. 1. Schematic diagram of ICP reactor equipped with VUVAS system employing the MHCL; (a) top view and (b) side view.

ing sample was set on the middle of electrode at 17.5 cm below the quartz window. The sample used as an organic low k film is FLARETM of which structure is shown in Fig. 2. The vacuum ultraviolet (VUV) light from MHCL was made parallel and introduced into the chamber through MgF₂ lens. The detailed structure of MHCL was described in Ref. 7. The VUV light passing once through the plasma at 10 cm above the substrate was focused by MgF₂ lens on the slit of a vacuum ultraviolet monochromator (Acton Research Corp., ARC VM-520) by MgF₂ lens and detected by a photomultiplier tube. The signal was recorded with a digital oscilloscope and averaged by a personal computer. The transition lines used for absorption measurements were a Lyman α at 121.6 nm for H atom, and $^4P_{5/2} - ^4S_{3/2}^0$, $^4P_{3/2} - ^4S_{3/2}^0$ and $^4P_{1/2} - ^4S_{3/2}^0$ at 120.0 nm for N atom. In order to calculate the absolute density in VUVAS measurement, it is necessary to estimate background absorption by some other molecules and radicals produced in the plasma.⁹ The background absorption was evaluated by the broad peak from Ar excimer at 122.5 nm.

Ionic species were measured by quadrupole mass spectrometer (QMS). The mass spectrometer (ANELVA, AQA-360) was positioned at the wall of chamber as shown in Fig. 1. The inside of the mass spectrometer was pumped by a 50

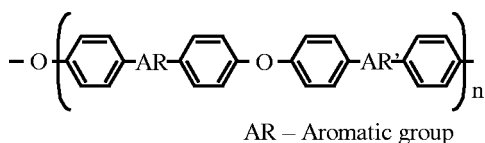


FIG. 2. Chemical structure of the FLARETM.

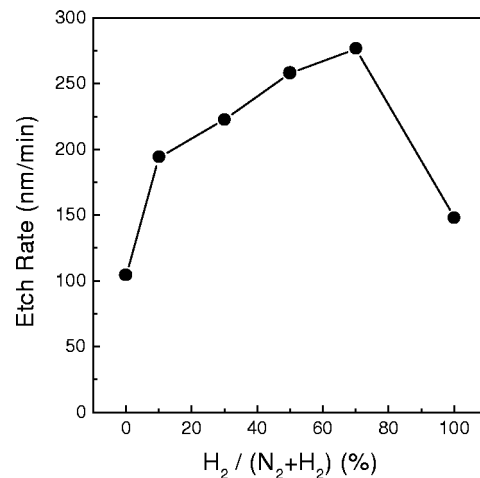


FIG. 3. Etch rate of FLARETM as a function of the flow rate ratio of H₂/(N₂+H₂).

l/s turbo-molecular pump. A monochromator (BENTHAM, M300) with a wavelength resolution of 0.4 nm was used for optical emission spectroscopy (OES) measurement. A 35 GHz microwave interferometer (NIHON KOSHUHA, MPI-1035J) was used to measure the electron densities (N_e).

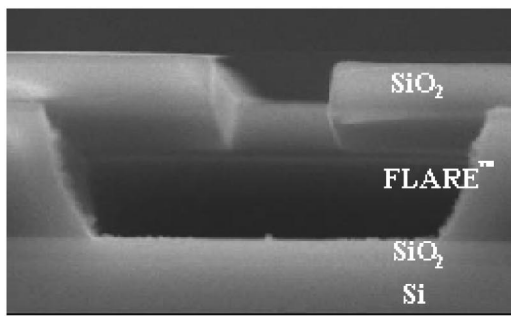
The etching conditions were maintained at a radio frequency (rf: 13.56 MHz) power of 1 kW, a total pressure of 2 Pa, and a total flow rate of 100 sccm. The self-bias voltage (V_{dc}) was fixed at -500 V by adjusting the rf bias power (1.6 MHz). The cross section of etching profile was observed by using a scanning electron microscope (SEM, HITACH S-4300). In order to obtain information of the composition on the etched surface, x-ray photoelectron spectroscopy (XPS) was employed.

III. RESULTS AND DISCUSSION

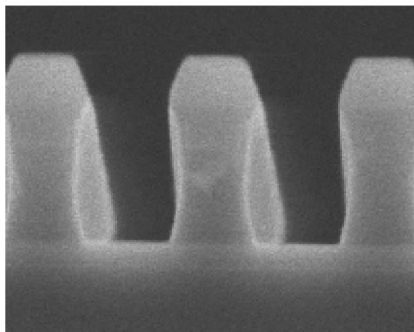
A. Employing N₂/H₂ plasma

Figure 3 shows the etch rate of FLARETM as a function of the flow rate ratio of H₂ gas to the sum of N₂ and H₂ gases, H₂/(N₂+H₂). The etching was carried out on the blanket film of FLARETM, and the etch rate was determined with a stylus profilometer by measuring the step height. As the flow rate ratio H₂/(N₂+H₂) increased, the etch rate increased, reached the maximum of 280 nm/min at H₂/(N₂+H₂)=0.7 (N₂/H₂=30/70 sccm), and then decreased at H₂/(N₂+H₂)=1 (N₂/H₂=0/100 sccm). These behaviors of etch rates are almost similar to the results reported previously elsewhere.³

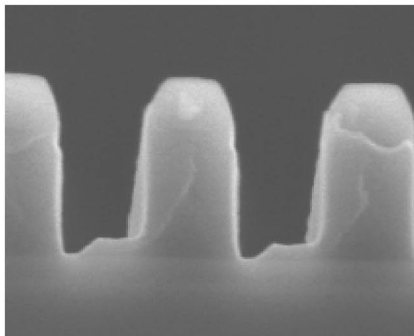
The patterned sample, which has the pattern size of 0.3 μm line and space structure, was etched under similar conditions to those used to etch blanket FLARETM. The sample used in this experiment consists of Photo-Resist/SiO₂/FLARETM/SiO₂ stacked structure. The thickness of hard mask, SiO₂, is 200 nm and that of FLARETM is 500 nm. In this case, however, substrate temperature was relatively high. Figure 4 shows the cross-sectional SEM images of the samples etched at various flow rate ratios. The sample etched at H₂/(N₂+H₂)=1 (N₂/H₂=0/100 sccm) had a large side etch as shown in the etched profile of Fig. 4(a). As the H₂



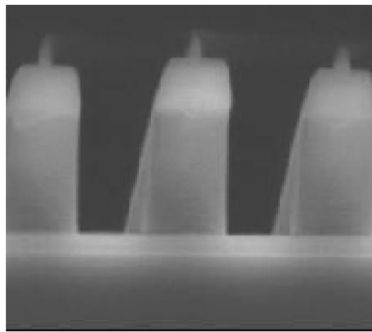
(a) $N_2/H_2 = 0/100$ sccm



(b) $N_2/H_2 = 95/5$ sccm



(c) $N_2/H_2 = 100/0$ sccm



(d) $N_2/H_2 = 85/15$ sccm

FIG. 4. SEM image of the etched profile of FLARE™ at ICP power of 1 kW, bias voltage (V_{dc}) of -500 V, total pressure of 2 Pa; (a) $N_2/H_2 = 0/100$ sccm, (b) $N_2/H_2 = 95/5$ sccm, (c) $N_2/H_2 = 100/0$ sccm, and (d) $N_2/H_2 = 85/15$ sccm.

flow rate ratio decreased, the etched profile became anisotropic from isotropic. At the condition of high N_2 flow rate ratio ($N_2/H_2 = 95/5$ sccm), the bowing profile was observed in Fig. 4(b). In these conditions where substrate temperature

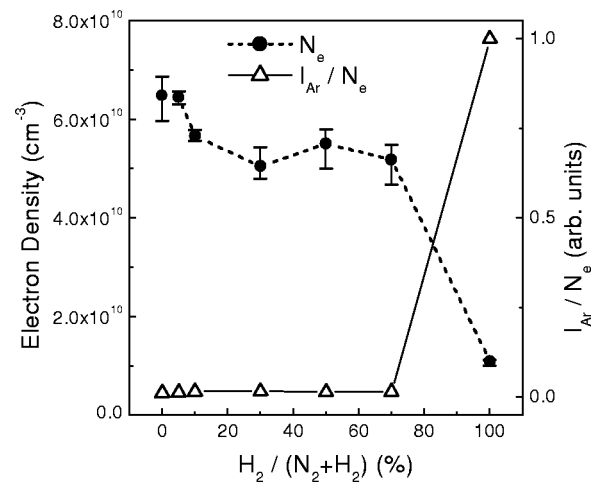


FIG. 5. Electron density measured by microwave interferometer and I_{Ar}/N_e as a function of the flow rate ratio of $H_2/(N_2+H_2)$.

was relatively high, the anisotropically etched profile was not obtained. At $N_2/H_2 = 100/0$ sccm, anisotropic profile was obtained. However, etch rate was low in this case, and the surface degradation on the bottom of pattern due to larger ion bombardment was observed in Fig. 4(c). When the substrate temperature was decreased by about $20^\circ C$ compared to these conditions, the etched profile was improved in the case using N_2/H_2 plasma. As shown in Fig. 4(c), at the condition of high N_2 flow rate ratio ($N_2/H_2 = 85/15$ sccm), highly anisotropic profile without surface degradation was successfully obtained.

To clarify these behaviors of etch rate and change of etched profiles, the plasma diagnostics were performed in etching plasma of organic low k film. Figure 5 shows electron densities N_e in N_2/H_2 plasmas measured by a microwave interferometer as a function of the flow rate ratio. The relative density of high-energy electrons, which was estimated from the Ar emission line (750.4 nm) intensity (I_{Ar}) divided by N_e , is also plotted in Fig. 5. In order to obtain the information on the density of high-energy electrons, a small amount of Ar (1%) was added to the etching plasma. The threshold energy of the electron impact excitation of Ar is 13.5 eV. The ratio of Ar emission intensity to N_e indicated the relative density of high-energy electrons above 13.5 eV which would contribute to dissociation of N_2 and H_2 . The plots in the figure indicate the averages of five measurements, and the error bars correspond to the maximum and minimum values. The electron density in the pure N_2 plasma is the highest. In the N_2/H_2 plasmas, the electron density and the relative density of high-energy electrons were almost constant in spite of the change of flow rate ratio. The electron density drastically decreased in H_2 plasma, and the relative density of high-energy electrons increased remarkably. This might be due to the large total ionization cross section of N_2 , which is about 2.5 times larger than that of H_2 .¹⁰

In order to obtain the information on ionic species generated in the N_2/H_2 plasma, quadrupole mass spectroscopy in the mass number of 1–50 amu was performed in both cases without sample and during sample etching. An electron impact energy of the ionizer was set at 0 eV during the mea-

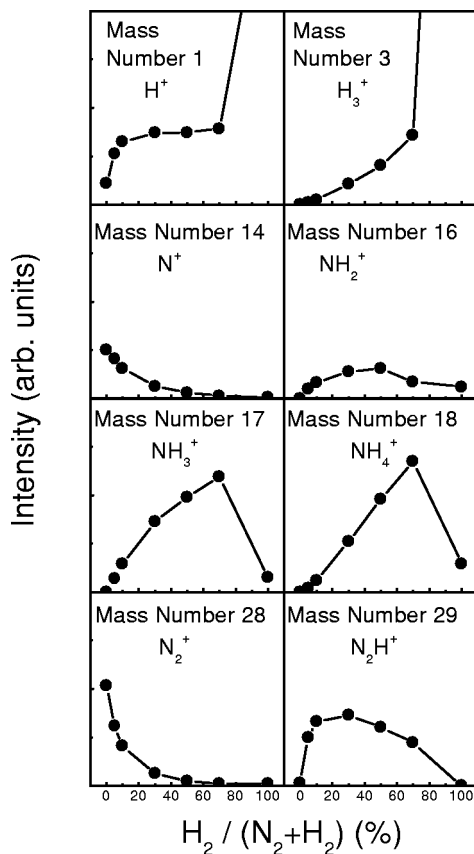


FIG. 6. Intensities of main mass numbers by QMS as a function of the flow rate ratio of $H_2/(N_2+H_2)$.

measurement of ionic species. Figure 6 shows intensities of main mass numbers generated in N_2/H_2 plasma without sample as a function of the flow rate ratio $H_2/(N_2+H_2)$. The behaviors of intensities of mass numbers 17 (NH_3^+), 18 (NH_4^+), and 29 (N_2H^+ ion), reached their maximum values nearby the center of the flow rate ratio of $H_2/(N_2+H_2)$, and were similar to the behavior of etch rate. Therefore, it is supposed that NH_3^+ , NH_4^+ , N_2H^+ ions contributed to the high rate etching of FLARETM in N_2/H_2 plasmas. During etching of samples, on the other hand, strong signal intensities from C_x

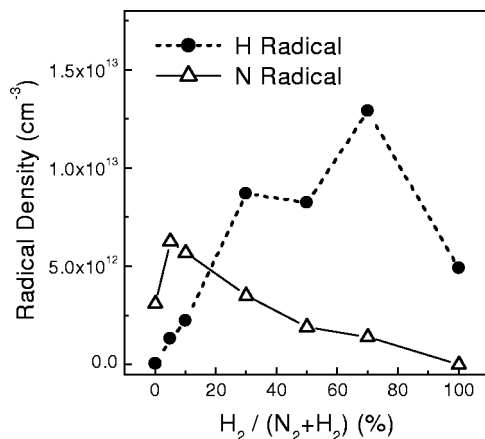


FIG. 7. H and N radical densities as a function of the flow rate ratio of $H_2/(N_2+H_2)$ employing VUVAS technique.

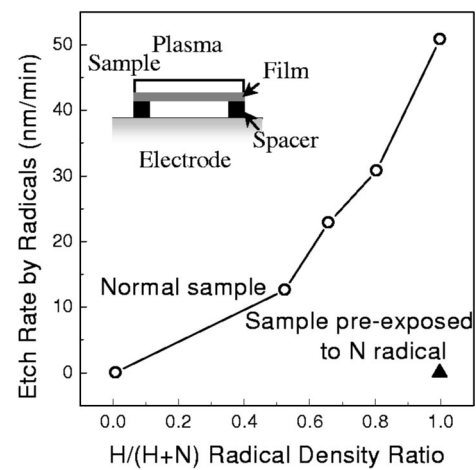
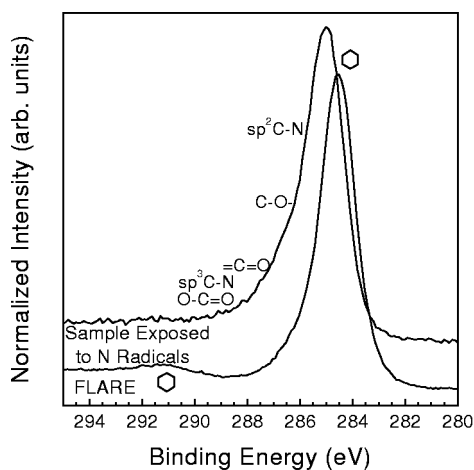


FIG. 8. Etch rate through radical reaction as a function of H and N radical densities ratio.

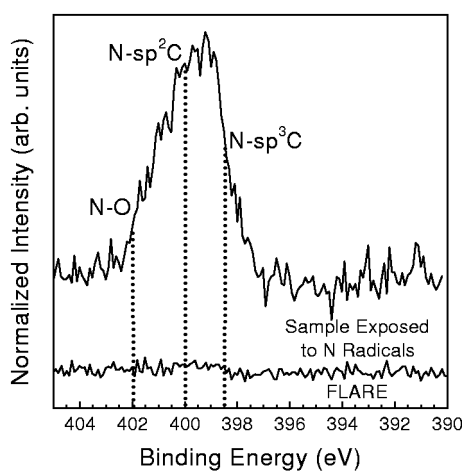
H_y^+ (hydrocarbon) ions such as CH_3^+ ion were observed in the pure H_2 plasma, and the signals from CN compound ions were observed in the pure N_2 plasma (date not shown). In the N_2/H_2 plasma, both $C_xH_y^+$ and CN compound ionic peaks were observed. As a result of OES measurement, emission from CN (388.3 nm) was observed during the etching of organic low k film. These results indicate that CN compounds such as HCN and C_xH_y , such as CH_4 of relatively low vapor pressure will be generated as by-products in H_2/N_2 plasma.

Figure 7 shows N and H radical densities measured employing VUVAS technique as a function of flow rate ratio $H_2/(H_2+N_2)$. The N radical densities were of the order of 10^{12} cm^{-3} , and increased gradually with increasing the N_2 flow rate ratio. The dissociation fraction of N_2 was 1.3% in the pure N_2 plasma. Since the behavior of N radical densities is much different from that of FLARETM etch rate, N radical would not contribute to the etching of FLARETM. As the flow rate ratio $H_2/(H_2+N_2)$ increased, the absolute H atom densities increased, and reached the maximum of $1.3 \times 10^{13} \text{ cm}^{-3}$ at $H_2/(H_2+N_2)=0.7$. The dissociation fraction of H_2 was 0.9% in the pure H_2 plasma. The behaviors of H radical and N radical densities were rather different from those of $H\alpha$ (656.3 nm) and N (673.7 nm) emission intensities, respectively. On one hand, the behavior of H radical density was similar to that of etch rate. Therefore, H radicals were considered to contribute dominantly to the etching of FLARETM in both N_2/H_2 and pure H_2 plasmas.

As shown in Fig. 5, the electron density was drastically increased by the addition of a little amount of N_2 gas to the H_2 gas, since the total ionization cross section of N_2 was larger than that of H_2 . Therefore, dissociation of H_2 was enhanced to generate more H radicals, which contributed to the etching of organic low k film. On the other hand, ignoring the negative ion densities in the plasma, the electron density is estimated to be equal to the total ion density. The ion bombardment by the increased total ion and especially relatively heavier ions such as $N_2H_x^+$ and NH^+ will enhance the etching reaction on the film surface. As a result, the H



(a) C1s



(b) N1s

FIG. 9. Normalized C 1s (a) and N 1s (b) electron spectra of sample surface exposed to N radicals and FLARE™.

radical density and the etch rate of organic low k film reached maximum at $N_2/H_2 = 30/70$ sccm.

Figure 8 shows the etch rate through the surface reaction with radicals as a function of the density ratio of H radicals to the sum of H and N radicals, $H/(H+N)$, measured by the VUVAS shown in Fig. 7. In order to make clear the roles of radicals on the etching of organic low k films, the etching of FLARE™ was carried out without the aid of ionic species by setting the surface of films upside down so that only radicals would reach the film surface through the spacers, as shown in the inset of Fig. 8. The etching was not observed in the case using pure N_2 plasma and the etch rate increased with the increase in flow rate of H_2 in the mixture. Therefore, it is suggested that the N radicals cannot contribute to etch organic low k films without ion bombardments, and that the H radicals are dominant etching species. The sample exposed to the N radicals was set in the configuration as shown in the inset of Fig. 8, and was etched by the H radicals again. However, the sample exposed to N radicals was not etched by H radicals at all, which is indicated by the closed triangle plot in Fig. 8. The XPS analysis was applied to the evalua-

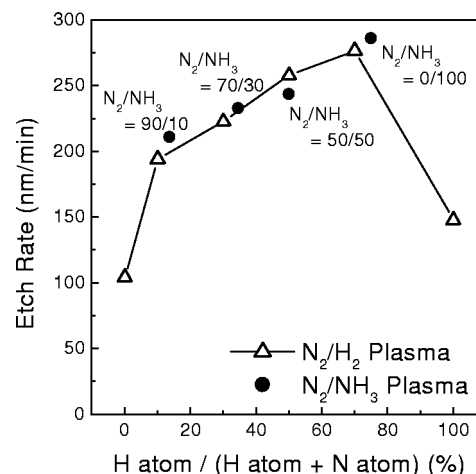


FIG. 10. Etch rate of FLARE™ as a function of H atom/(H atom + N atom) in feed gases. The open triangles (Δ) and filled circles (\bullet) represent the etch rate in N_2/H_2 plasma and in N_2/NH_3 plasma, respectively.

tion of sample surface before and after the exposure to the N radicals. The XPS (FISONS, Escalab-220i) measurement was performed by using $Mg K_{\alpha}$ radiation (1242.6 eV) with a scanning energy step of 0.1 eV. Figures 9(a) and 9(b) show the normalized C 1s and N 1s electron spectra of FLARE™ surface before and after being exposed to N radicals. These spectra were obtained at take-off angles of 90° and calibrated by $Ag 3d_{3/2}$ peak at 368.3 eV. The C 1s spectrum of original FLARE™ has a symmetric peak centered at 284.5 eV attributed to the benzene ring and the broad peak around 291.5 eV which is called shake-up satellite. This shake-up satellite is typical of hydrocarbon polymers with pendant aromatic groups. The C 1s spectrum of sample exposed to N radicals has a broad and asymmetric peak at higher binding energies as compared with C 1s spectrum of original FLARE™. This is because the C 1s peak consists of many elements.¹¹ The N 1s spectrum of the sample exposed to N radicals has a broad peak corresponding to some bonding configurations related to nitrogen atoms. The N 1s peak consists of three contributions.^{12,13} The two main contributions are centered at 398.5 and 400.0 eV, which are attributed to sp^3 -hybridized carbon (N- sp^3C) and sp^2 -hybridized carbon (N- sp^2C), respectively. The minor contribution at 402.0 eV corresponds to N-O bonds, which is probably related to incorporation of oxygen into the sample due to the exposure to atmosphere before XPS measurement. From these results, CN layer was formed on the surface of the sample exposed to N radicals. Consequently, the sample exposed to N radicals was not etched as shown in Fig. 10. This result was interpreted as that the CN layer formed by N radicals protected against etching by H radicals. This CN protection layer at sidewall must be effective for the formation of anisotropic profile under the condition of high N_2 concentration with a small addition of H_2 as shown in Fig. 4(c).

B. Employing N_2/NH_3 plasma

It was reported that high rate etching was obtained employing NH_3 plasma compared to the case employing N_2/H_2

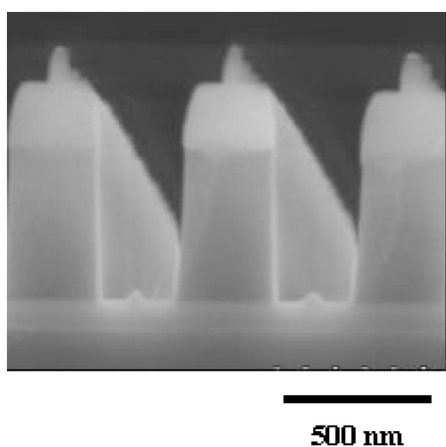


FIG. 11. SEM image of the etched profile of FLARE™ at ICP power of 1 kW, bias voltage (V_{dc}) of -500 V, pressure of 2 Pa, $N_2/NH_3=90/10$ sccm.

plasma.⁴ In this section, organic low k film etching using N_2/NH_3 plasma was investigated in comparison with the result of N_2/H_2 plasma etching.

Figure 10 shows the etching characteristics of FLARE™ as a function of the concentration ratio of H atom to the sum of H atom and N atom in feed gases, H atom/(H atom + N atom). In this figure, the open triangles (Δ) represent the etch rate using N_2/H_2 plasma as shown in Fig. 3 and filled circles (\bullet) represent the etch rate using N_2/NH_3 plasma, respectively. In the case using N_2/H_2 plasma, as the atomic concentration ratio H atom/(H atom + N atom) increased, the etch rate increased, reached the maximum of 280 nm/min at H atom/(H atom+N atom)=0.7 ($N_2/H_2=30/70$ sccm), and then decreased. In the N_2/NH_3 plasma, as the ratio H atom/(H atom+N atom) increased, the etch rate increased, and reached the maximum of 290 nm/min at H atom/(H atom+N atom)=0.75 ($N_2/NH_3=0/100$ sccm). It was found that the etch rate depended only on the concentration ratio of H atom in feed gases, and was independent of the kind of gases under these etching conditions.

Figure 11 shows a SEM image of etched profile employing N_2/NH_3 plasma at the atomic concentration ratio H atom/(H atom+N atom)=0.14 ($N_2/NH_3=90/10$ sccm) in the feed gas, a total pressure of 2 Pa, ICP power of 1 kW, bias voltage of -500 V. This concentration ratio was similar to the case used for the etching employing N_2/H_2 gas as shown in Fig. 4(c). By adjusting the concentration ratio of H atom in feed gases, the etched profile with the same shape was obtained in both N_2/H_2 and N_2/NH_3 plasmas.

Figure 12 shows N and H radical densities measured using VUVAS technique as a function of the concentration ratio H atom/(H atom + N atom) in the feed gases. In this figure, which was rearranged from the result shown in Fig. 7, the open symbols (\circ , Δ) represent H and N radical densities in N_2/H_2 plasma, respectively. The filled symbols (\bullet , \blacktriangle) represent H and N radical densities in N_2/NH_3 plasma. The H and N radical densities were of the order of 10^{12} – 10^{13} cm^{-3} in N_2/NH_3 plasma. It was confirmed from the result in Fig. 12 that the behavior of H and N radical densities depended only on the concentration ratio of H atom in the feed gases, and was independent of the kind of gases.

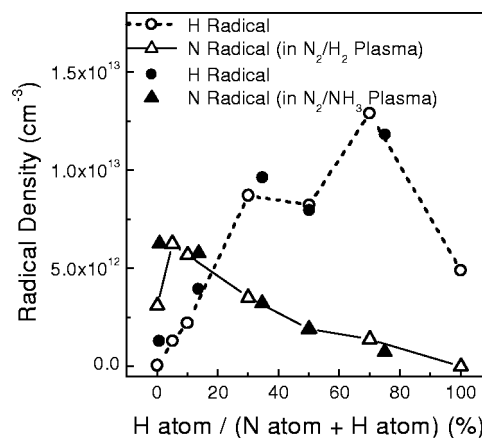


FIG. 12. H and N radical densities as a function of H atom/(H atom+N atom) in feed gases employing VUVAS technique. The open symbols (\circ , Δ) represent H and N radical densities in N_2/H_2 plasma, respectively. The filled symbols (\bullet , \blacktriangle) represent H and N radical densities in N_2/NH_3 plasma.

From these results, it was indicated that the etching characteristics such as etch rate and etched profile of organic low k film depend strongly on the N and H radical densities and their ratio under our etching conditions. The ratio of H and N radical densities would be important for the high-performance etching of organic low k film employing N_2/H_2 and N_2/NH_3 plasmas.

IV. CONCLUSION

The organic low k films were etched in the inductively coupled plasma employing the mixtures of N_2/H_2 and N_2/NH_3 . The etch rate obtained reaches the maximum at the ratio $H_2/(H_2+N_2)=0.7$. The behaviors of absolute densities of H and N radicals were investigated during the etching employing VUVAS technique with microdischarge hollow-cathode lamp. The correlation between etching characteristics and behaviors of H and N radicals were clarified as follows.

(1) N_2 gas addition to the H_2 gas was found to increase the electron densities, resulting in the increase of H radical density and ion bombardment. As a result, the etch rate of organic low k film was increased.

(2) The etching through radicals without the aid of ion bombardment was carried out and H radicals were found to be dominant species for organic low k film etching, while N radicals could not etch without ion bombardments. Moreover, N radicals were found to be effective for the formation of protection layer on the sidewall against the etching by the H radicals. On the other hand, N radicals and N_2^+ ions would form CN compound on the bottom of pattern, which cause the degradation of etched profile.

(3) The etching characteristic employing N_2/NH_3 plasma was almost the same as that employing N_2/H_2 plasma, on condition that the atomic concentration ratio of H and N is common in the feed gases used. The behavior of H and N radical densities depended on the concentration ratio in feed gas, and was independent of the kind of gases. The ratio of H

and N radical densities would be important for the etching of organic low k film employing N–H plasmas.

ACKNOWLEDGMENTS

The authors would like to thank Rasa Industries, Ltd., for providing the FLARE™ samples. They would also like to thank Dr. K. Miyata, Dr. T. Tatsumi, and Dr. S. Kadomura of Sony Corporation for useful discussions. This work is partially supported by NEDO.

¹M. R. Baklanov, S. Vanhaelemeersch, H. Bender, and K. Maex, *J. Vac. Sci. Technol. B* **17**, 372 (1999).

²S. A. Vitale, H. Chae, and H. H. Sawin, *J. Vac. Sci. Technol. A* **18**, 2770 (2000).

³M. Fukasawa, T. Hasegawa, S. Hirano, and S. Kadomura, in *Proceedings of Symposium on Dry Process*, edited by Y. Horiike (Waseda University, Tokyo, Japan, 1998), pp. 175–182.

⁴M. Fukasawa, T. Tatsumi, T. Hasegawa, S. Hirano, K. Miyata, and S. Kadomura, Ref. 3, 1999, p. 221–226.

⁵T. E. F. M. Standaert, P. J. Matsuo, S. D. Allen, G. S. Oehrlein, and T. J. Dalton, *J. Vac. Sci. Technol. A* **17**, 741 (1999).

⁶T. E. F. M. Standaert, E. A. Joseph, G. S. Oehrlein, A. Jain, W. N. Gill, P. C. Wayner, Jr., and J. L. Plawsky, *J. Vac. Sci. Technol. A* **18**, 2742 (2000).

⁷S. Takashima, A. Kono, M. Ito, K. Yoneda, M. Hori, and T. Goto, *Appl. Phys. Lett.* **75**, 3929 (1999).

⁸S. Takashima, S. Arai, A. Kono, M. Ito, K. Yoneda, M. Hori, and T. Goto, *J. Vac. Sci. Technol. A* **19**, 599 (2001).

⁹K. Tachibana and H. Kamisugi, *Appl. Phys. Lett.* **74**, 2390 (1999).

¹⁰W. Hwang, Y.-K. Kim, and M. E. Rudd, *J. Chem. Phys.* **104**, 2956 (1996).

¹¹K. B. Boyd, D. Marton, S. S. Todorov, A. H. Al-Bayati, J. Kuliki, R. A. Zuhr, and J. W. Rabalais, *J. Vac. Sci. Technol. A* **13**, 2110 (1995).

¹²W. T. Zheng, E. Broitman, N. Hellgren, K. Z. Xing, I. Ivanov, H. Shöström, L. Hultman, and J. E. Sundgren, *Thin Solid Films* **308–309**, 223 (1997).

¹³D. Briggs and M. P. Seah, *Practical Surface Analysis by Auger and X-Ray Photoelectron Spectroscopy* (Wiley, Sussex, 1984).